# Concentration effects on aqueous lithium chloride solutions. Molecular dynamics simulations and x-ray scattering studies

**ARTICLE** *in* JOURNAL OF MOLECULAR LIQUIDS · SEPTEMBER 2014

Impact Factor: 2.52 · DOI: 10.1016/j.molliq.2014.04.018



**1 AUTHOR:**

Salah Nasr
University of Monastir
**42** PUBLICATIONS **350** CITATIONS

SEE PROFILE

Journal of Molecular Liquids 197 (2014) 77–83

Contents lists available at ScienceDirect

Journal of Molecular Liquids

journal homepage: www.elsevier.com/locate/molliq

# Concentration effects on aqueous lithium chloride solutions. Molecular dynamics simulations and x-ray scattering studies

Salah Bouazizi, Salah Nasr *

*Laboratory of Material Physico-chemistry, Department of Physics, Faculty of Sciences, University of Monastir, Monastir 5019, Tunisia*

ARTICLE INFO

*Article history:*
Received 4 January 2014
Received in revised form 10 April 2014
Accepted 18 April 2014
Available online 5 May 2014

*Keywords:*
Aqueous LiCl solutions
Molecular dynamics
Structure factor
X-ray
Diffusion coefficients

ABSTRACT

Molecular dynamics simulations have been performed on aqueous LiCl solutions over a wide range of salt concentrations, using a flexible SPC/E water model. The resulting molecular dynamics structure factors agree remarkably with recently published x-ray ones. The diffusion coefficients of both ions and water decrease with increasing salt concentration. The self-diffusion coefficients of lithium and chloride are nearly equal at higher salt concentration, showing that large clusters of ions move as an entity. The deduced reorientational correlation time for the dipole moment speeds up as the salt concentration increases, indicating the presence of an angular jump model. The dielectric constant decreases with increasing salt concentration.



## 1. Introduction

Water is ubiquitous on the earth and in living organisms [1], it has extraordinary microscopic properties uncommon for the majority of liquids [2], a good part of which comes from intermolecular hydrogen bonding. An understanding of the orientational dynamics of water is essential in a wide range of processes, such as the rearrangement of the water hydrogen-bond network [3], the biomolecular hydration and the drag–protein recognition [4]. In most cases, water does not exist as a pure substance, but rather it contains dissolved salts. The dielectric properties of water influence the electrolyte and therefore the salvation of ions in aqueous solutions [5].

Laage and Hynes [6,7] have proposed a molecular mechanism of water reorientation which leads to the rupture and the creation of hydrogen-bonding phenomenon in concrete terms. In the diffusive model, water molecule redirection is achieved by infinitesimal steps, whereas in the extended jump model, the exchange of H-bonding, effectuated in a very short time, is realized by large amplitude angular jumps.

The ionic aqueous solutions play a central role in environmental and industrial processes like microbiology [8], and oxidation of chemical and biochemical wastes [9]. As a consequence, they have been frequently chosen as subjects of experimental and theoretical investigations. In particular $Li^+$ and $Cl^-$, which are essential for biophysical systems, continue to attract a particular attention for many reasons. For example, ion lithium is, one of the most simple metal ions playing widespread and diverse roles in biological, medical, and technical application [10].

Recently [11,12], we have presented a structural analysis of aqueous LiCl solutions by combining x-ray scattering and MD simulations. In that study, as an essential point, it was shown that the ion-pairing process increases with increasing salt concentration. Simultaneously, the degree of hydrogen bonding in liquid water clearly decreases, whereas the coordination number of water in solution increases in comparison to that of the pure fluid. To get more insight on the properties of aqueous LiCl solutions, we extend in this paper our MD investigation, to study the effects of salt concentration on dynamical properties of ions and water. In addition, all the partial correlation functions and structure factors of the systems are deduced. A comparison between experimental results and theoretical ones, using a flexible SPC/E water model, is then addressed.

The outline of this paper is the following. The computational details of the MD simulations are given in Section 2. The computed structure factors, pair correlation functions, velocity autocorrelation functions, self-diffusion coefficients, reorientational correlation times and dielectric constants are determined in Section 3. The conclusion and final remarks are presented in Section 4.

## 2. Computational details

The molecular dynamics formalism was described elsewhere [13]. Only a brief outline will be given here. In all simulations, the water molecules are characterized by the flexible SPC/E potential and the ions are modeled as charged Lennard-Jones particles. The values of the potential parameters $q_i$, $\sigma_i$, and $\varepsilon_i$ for all particles are summarized in Table 1 [14–16]. A cubic box of 256 particles including water molecules and ions is chosen, and periodic boundary conditions with minimum image convention were used. The initial configurations of water molecules

* Corresponding author.
*E-mail address:* salah_nasr1@yahoo.fr (S. Nasr).

http://dx.doi.org/10.1016/j.molliq.2014.04.018
0167-7322/

**Table 1**
Values of Lennard-Jones and electrostatic interaction potential parameters; e represents the magnitude of electronic charge.

| Atom/ion | Charge (e) | ε (kJ/mol) | σ (Å) | Ref. |
|---|---|---|---|---|
| O | −0.8476 | 0.6502 | 3.169 | [14] |
| H | +0.4238 | 0.0 | 0.0 | [15] |
| $Li^+$ | +1 | 0.6904 | 1.505 | [16] |
| $Cl^-$ | −1 | 0.4184 | 4.401 | [16] |

and ions are obtained by a random displacement of the particles in the box, which the length is chosen to match the experimental density. The Lorentz–Berthelot combining rules [17] are used to describe the cross-interactions, and the long-range Coulomb forces are calculated using the Ewald summation method [18]. The convergence parameter is $\alpha = \frac{5.36}{L}$ and the maximum k in the reciprocal space is such that $k^2_{max} \leq 27$. The non-Coulomb short range interactions were truncated using a spherical cut-off distance equal to the half of the cell length. The weak coupling scheme according to Berendsen et al. [19] is applied.

We have performed a series of sufficiently long MD simulations of aqueous LiCl solutions at different salt concentrations, ranging from 0.5 to 6 m. The simulation parameters of the studied systems are reported in Table 2. The equations of motion are integrated using the Verlet Leap-Frog algorithm and the initial velocities are generated assuming a Maxwell–Boltzmann distribution.

## 3. Results and discussion

The computed densities of aqueous LiCl solutions at different concentrations are given in Table 2 together with measured ones. There is a small difference between the experimental and theoretical values. The different contributions into the total energy are also presented in Table 2. One can see that water–water interaction energy $E(H2O\cdots H2O)$ is increasing with an increase of the salt concentration. This effect takes place mainly due to the disruption of the hydrogen bonds. The ion–water interactions $E(Li^+\cdots H_2O)$ and $E(Cl^-\cdots H_2O)$ both become weaker upon an increase of the salt concentration. This is due to the influence of other ions on the hydrated shell. The increase of the ion–water energy is compensated by the decrease of the ion–ion energy.

In our previous studies [11] and [12], our investigations are focused on the local structure of aqueous LiCl solutions through pair correlation functions as deduced respectively from x-ray scattering and MD simulation. In that study, some simplifying hypotheses are constructed: i) All the X–H (where X = H, O, $Li^+$, $Cl^-$) correlations are omitted since the contribution of such interactions to the x-ray scattered intensity are weak particularly at high q values, and ii) the contribution of ion–ion interactions which occur in MD results at relatively high distances is also omitted since no signature of these interactions appears in the x-ray pair correlation functions. However, the theoretical model which we have considered in these studies and which takes into account the more scattering element gives reasonable concordance with x-ray results. In this study, in order to show more reliability for our computational model, we calculate the intermolecular structure factors of each system as the weighted average of all partial ones:

$$S(Q) = \frac{\sum_{\alpha,\beta} c_\alpha c_\beta f_\alpha(Q) f_\beta(Q) S_{\alpha\beta}(Q)}{\sum_{\alpha,\beta} c_\alpha c_\beta f_\alpha(Q) f_\beta(Q)} \quad (1)$$

where $c_\alpha = \frac{N_\alpha}{N}$ is the concentration of α specie, $f\alpha(Q)$ is the x-ray form factor and $S_{\alpha\beta}(Q)$ is the partial static structure factor directly deduced from MD simulation via the relation:

$$S_{\alpha\beta}(Q) = 1 + \frac{4\pi\rho_0}{Q}\int_0^\infty r\left[g_{\alpha\beta}(r) - 1\right]\sin(Qr)dr \quad (2)$$

where $\rho_0$ denotes the atomic number density of the system.

In a similar way, the intermolecular pair correlation function $g_L(r)$ of each system is the weighted average of the partial ones [13]:

$$g_L(r) = \frac{\sum_{\alpha,\beta} c_\alpha c_\beta f_\alpha(Q) f_\beta(Q) g_{\alpha\beta}(r)}{\sum_{\alpha,\beta} c_\alpha c_\beta f_\alpha(Q) f_\beta(Q)}. \quad (3)$$

Fig. 1(A) shows the MD and the x-ray structure factors S (Q) for each system. It can be noted that the agreement between the calculated and experimental data is quite good. The mean feature of the experimental pair correlation function g(r) (Fig. 1(B)) is also well reproduced by the calculated ones. Particularly, calculated and experimental curves reveal a good concordance in the description of the development of the intermolecular interactions and the disruption of the water structure as a function of salt concentration.

To get an idea about the dependence of the system size on the structure factor and pair correlation functions, three different systems corresponding to C = 3 m and containing respectively 256, 526 and 1052 particles were used. In Fig. 2(A), we have drawn the MD structure factor and the corresponding pair correlation function of each system. Manifestly, the oscillatory character of the curves is slightly amplified whereas the intermolecular interactions are at the same positions Fig. 2(B).

The dynamical properties of the ions and water molecules can be examined via the velocity autocorrelation functions (VACFs). The normalized VACF, $Cv_i(t)$, for the ith particle is defined as:

$$Cv_i(t) = \frac{\langle v_i(t) v_i(o)\rangle}{\langle v_i(0)^2\rangle} \quad (4)$$

where $v(t)$ is the velocity of the ion at time t, and ⟨⟩ denotes an ensemble average.

**Table 2**
Simulation parameters and some physical properties of aqueous LiCl solutions. All the energies are given in kJ/mol.

| System | 1 | 2 | 3 | 4 | 5 |
|---|---|---|---|---|---|
| Number of $H_2O$ | 252 | 244 | 232 | 224 | 208 |
| Number of ions | 4 | 12 | 24 | 32 | 48 |
| Average box length (Å) | 19.62 | 19.50 | 19.38 | 19.25 | 19.02 |
| Salt concentration (m) | 0.5 | 1.5 | 3 | 4 | 6 |
| Experimental density ($g/cm^3$) | 1.013 | 1.043 | 1.074 | 1.101 | 1.156 |
| Calculated density ($g/cm^3$) | 1.012 | 1.041 | 1.069 | 1.097 | 1.0140 |
| $E_{tot}$ | −37.419 | −50.261 | −69.519 | −82.274 | −107.851 |
| $E(H_2O\cdots H_2O)/N_{H2O}$ | −46.295 | −37.812 | −28.530 | −21.219 | −9.873 |
| $E(Li^+\cdots H2O)/N_{Li+}$ | −747.065 | −635.616 | −531.318 | −500.260 | −473.438 |
| $E(Cl^-\cdots H2O)/N_{Cl-}$ | −579.860 | −559.575 | −380.826 | −363.511 | −335.840 |
| $E(Li^+\cdots Li^+)/N_{Li+}$ | 52.092 | 222.405 | 531.209 | 750.457 | 1189.953 |
| $E(Li^+\cdots Cl^-)/N_{Li+}$ | −262.053 | −714.522 | −438.051 | −1901.464 | −2812.687 |
| $E(Cl^-\cdots Cl^-)/N_{Cl-}$ | 51.342 | 220.302 | 529.551 | 762.873 | 1187.844 |

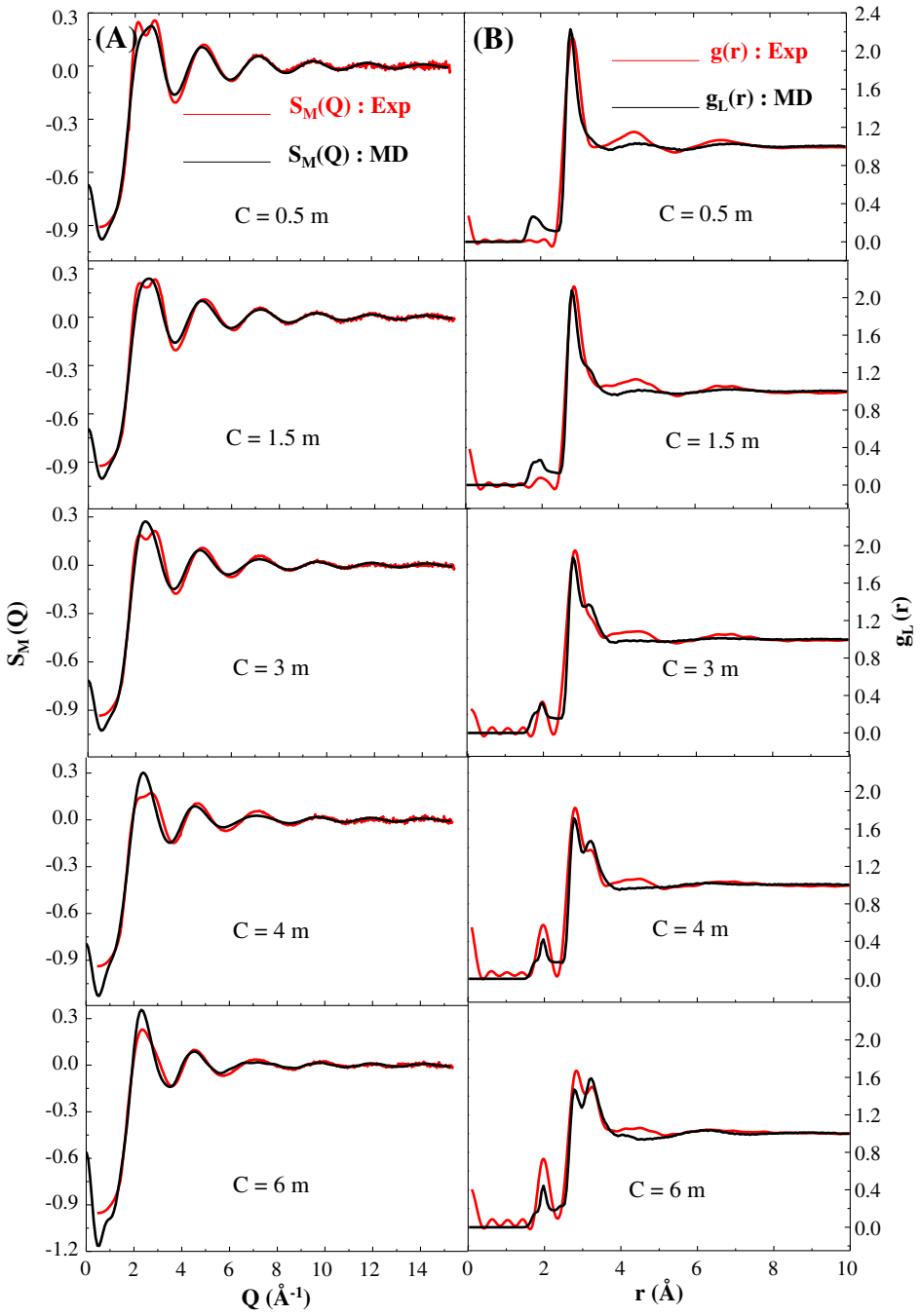


**Fig. 1.** (A) Comparison between x-ray structure factors of aqueous LiCl solutions and computed ones using SPC/E water model. (B) Comparison between x-ray pair correlation functions of aqueous LiCl solutions and computed ones using SPC/E water model.

The most common quantity to describe the dynamical behavior of a system is its diffusion coefficient D. For the ith particle, $D_i$ can be calculated from the VACFs according to the relation:

$$D_i = \frac{1}{3}\int_0^\infty (v_i(t)v_i(0))dt. \quad (5)$$

The translational self-diffusion coefficient can also be obtained from the long-time limit of the mean square displacement (MSD) by

$$D_i = \lim_{t\to\infty} \frac{\left\langle [r_i(t)-r_i(0)]^2 \right\rangle}{6t}. \quad (6)$$

As can be seen from Fig. 3, the VACFs' change in shape with the increase of the concentration. The oscillatory shapes of the curves characterize the oscillations of a particle in the cage formed by the molecules of the salvation shells, leading the particle to reverse the direction of its motion. We also observed a noticeable increase of the first minima (less becomes negative) in the case of water and $Cl^-$ with increasing salt concentration. In fact, the examination of the oxygen–oxygen pair correlation function (Fig. 4) shows a decrease of the height of the first peak with increasing salt concentrations, and a net shift of the first minimum which moves from about 3.425 Å for 0.5 m to 3.825 for 6 m solution. This leads to an increase of the water coordination number. The oscillations, at a short time, are more marked for $Li^+$ than $Cl^-$. This indicates that the probability for $Li^+$ to reverse its motion i.e., the extent of caging is more marked for $Li^+$ than $Cl^-$.

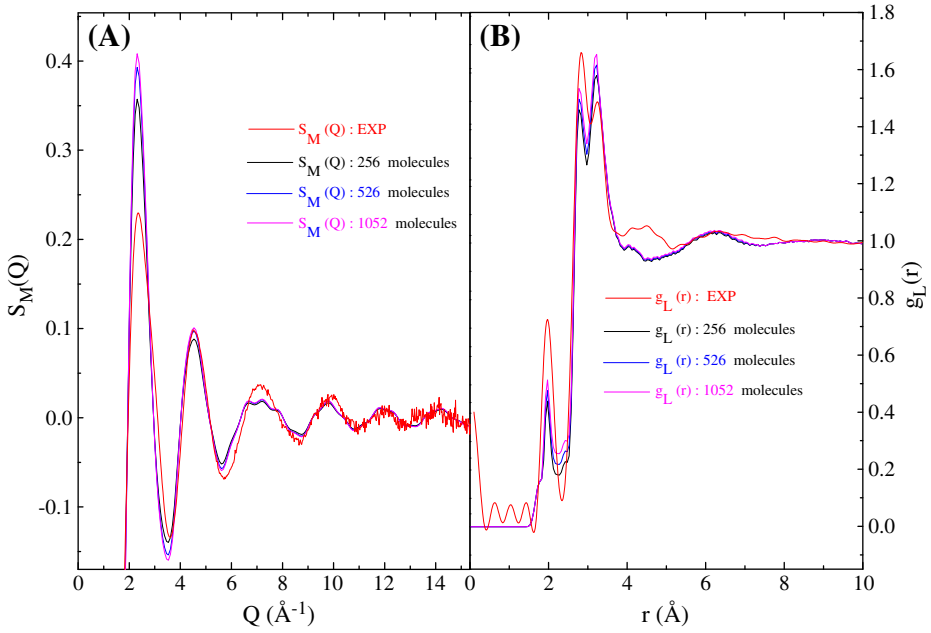


**Fig. 2.** (A) Comparison between x-ray structure factors of aqueous LiCl solutions and computed ones using SPC/E water model as a function of system size. (B) Comparison between x-ray pair correlation functions of aqueous LiCl solutions and computed ones using SPC/E water model as a function of system size.

Table 3 reports the self diffusion coefficients of water and both ions obtained by two different methods, i.e., from the VACF and MSD (Fig. 5). The self-diffusion coefficients from MSD curves are calculated from the slope, of the respective ones, in the range of 20–100 ps using Einstein's relation (Eq. (6)). One can see a good agreement between the results of the two methods. Our results clearly indicate that the diffusion coefficients for all species decrease with increasing salt concentration. This trend corroborates the conclusion of Egorov et al. [20] in their MD simulation of aqueous LiCl solutions that had used three different ion–water potentials.

Good agreement can be highlighted by comparing our results with corresponding ones from literature. For example the $D_{Li+}$ at 0.5 m and at 6 m, respectively equal to 1.07 and $0.259 \times 10^{-9}$ $m^2$ $s^{-1}$, are in good agreement with the results [20] 1.09 and $0.33 \times 10^{-9}$ $m^2$ $s^{-1}$ respectively at 0.16 and at 5.89 m. The latter study has been performed using the SPC/E water model and Dang potential for lithium–water interaction. In the same manner, a fair concordance is observed between our results at 0.5 m and those of Koneshan et al. [15] at infinite dilution ($D_{Li+} = 1.18 \pm 0.1 \times 10^{-9}$ $m^2$ $s^{-1}$) using the SPC/E water model at 298 K. The self diffusion coefficient of the SPC/E water model changes dramatically in magnitude as the solution becomes denser. Indeed $D_w$ decreases by 50% from 0.5 to 6 m. Over the same concentration range, the diffusion coefficient of water in NaCl [21] solutions also shows a decrease of an overall drop by 51.8%.

In the same range of concentrations, the $Li^+$ diffusion coefficients are smaller (Fig. 6) than the $Na^+$ ones deduced in our previous paper [21]. This result corroborates previous investigations [15,16,22] focused on aqueous ionic solutions at infinite dilution. Similarly, Chowdhuri and Chandra [23] found that the $D_{K+}$ is larger than the $D_{Na+}$. Although the crystallographic radii of alkali cations increase with atomic number ($Li^+ < Na^+ < K^+$), the diffusion coefficient observed in aqueous solutions increases with increasing ion size.

The difference between $D_{Li+}$ and $D_{Cl^-}$ decreases progressively as the salt concentration increases. At high salt concentrations, the two diffusion coefficients have to been found quite close to each other. This phenomenon can be explained by the formation of a cluster of these ions which tend to migrate together as a whole, leading also to a lower $D_{Li+}$ and $D_{Cl^-}$. This phenomenology is approved by analyzing the lithium–chloride pair correlation functions (Fig. 7). As shown in this figure, the probability of close $Li^+ \cdots Cl^-$ contact is very low at infinite dilution. However, the peak at about 2.47 Å corresponding to close $Li^+ \cdots Cl^-$ contact pair increases remarkably with increasing salt concentration. Simultaneously there is a clear decrease of the second and third ones, which proves the formation of pairing ions and a decrease of separated ones. Harsányi et al. [24,25] studied the structure of concentrated aqueous lithium chloride solutions. It was found that at the highest concentration, some counterions intrude into the first Li–H and Cl–O coordination shells. The cluster building, which is observed in highly concentrated solutions [26], is in broad agreement with our previous findings [21]. Koneshan and Rasaiah [5] found that the diffusion coefficients of $Na^+$ and $Cl^-$ ions, decrease with increasing electrolyte concentration. Also, they are nearly equal to each other in a one molal solution at 683 K, in which, the large cluster of sodium and chloride ions moves as an entity.

Molecular reorientational motions in liquids are usually analyzed through the time correlation functions:

$$C_l^{\beta}(t) = \left\langle P_l\left(\vec{u}_{\beta}(t) \cdot u_{\beta}(0)\right)\right\rangle \tag{7}$$

where $P_l$ refers to the lth Legendre polynomial and $\vec{u}_{\beta}$ is a unit vector along a given direction. We calculated $C_1^u(t)$ and $C_2^u(t)$ for a unit vector $\vec{u}_u$ along the molecular dipole moment direction, $C_1^u(t)$ is related to dielectric and NMR relaxation measurements.

In order to make a quantitative analysis of the rotational dynamics, we have evaluated the reorientational correlation times $\tau_l^u$ for the analyzed directions as the time integrals:

$$\tau_l^u = \int_0^{\infty} C_l^u(t)dt \tag{8}$$

where the $C_l^u(t)$ can be fitted by a multiexponential:

$$C_l^u(t) = \sum_{i=1}^{3} a_i \exp\left(\frac{-t}{\tau_i}\right) \tag{9}$$

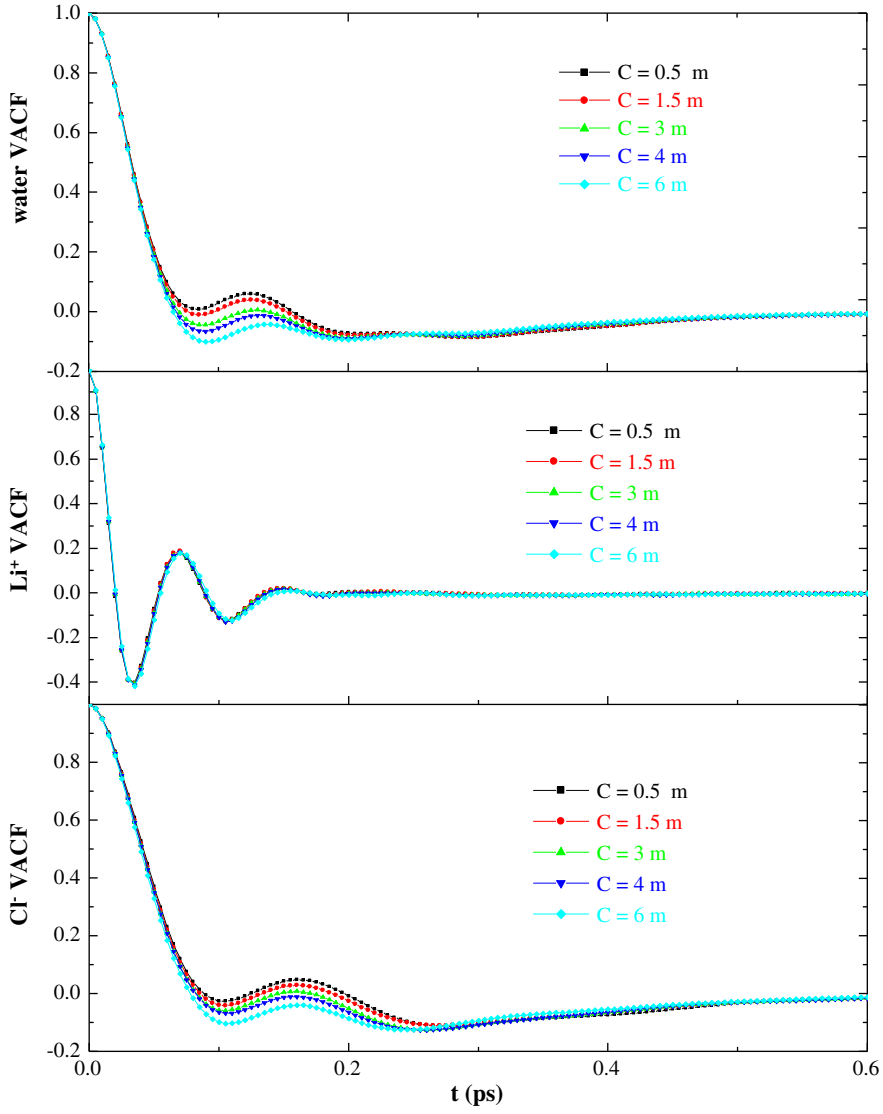


**Fig. 3.** The velocity autocorrelation functions for water (i.e. for the center of mass of the molecule), $Li^+$ and $Cl^-$ in aqueous LiCl solutions at different salt concentrations.

from which a reorientational correlation time can be obtained:

$$\tau_l^u = \frac{\sum_{i=1}^{3} a_i \tau_i}{\sum_{i=1}^{3} a_i}. \quad (10)$$

Table 3 reports the first and second reorientational times for the dipole moment. Unlike translational diffusion coefficients, the reorientational correlation time of dipole studied here shows an increase with salt concentration. The same trend has been observed by Chowdhuri and Chandra [23] in their study of aqueous NaCl and KCl solutions.

Instead of diffusive model suggesting that hydrogen-bond breaking and water molecule reorientation are involved successively, Laage and Hynes [6,7] have proposed a molecular mechanism of water reorientation which leads to the rupture and the creation of hydrogen-bonding phenomena in concrete terms, called jump model. Our study clearly shows that the ratio of the first and second orientational correlation times differs from 3, which probably indicates the presence of angular jumps.

The dielectric constant $\varepsilon_s$ of the fluid may be calculated according to the standard expression [27]

$$\varepsilon_s - 1 = \frac{4\pi}{3kTV}\left[\left\langle M^2\right\rangle - \langle M\rangle^2\right] \quad (11)$$

where M is the total dipole moment of the system, k is the Boltzmann constant, T is the temperature, and V is the volume. The calculated dielectric constant decreases (Table 3) from 73.279 at 0.5 m to 26.350 at 6 m. The reduction of the dielectric constant with increasing salt concentration is caused by the reduction of the orientational correlation between water molecules in the vicinity of ions. Similarly, Gallo et al. [28] have observed in their study of aqueous solutions of potassium chloride and fluoride that the hydrogen bond network of water is perturbed by the increasing concentration. For comparison, the dielectric constant at 0.5 m, 73.279, is smaller than the value for pure water, 73.5, deduced by using the same SPC/E [29] potential. Experimental measurements show that the dielectric constant of water decreases from 78 at zero salt concentration to 40 in 4 M NaCl, and that it can be decreased to as low as 18 in 13 M LiCl [30,31].

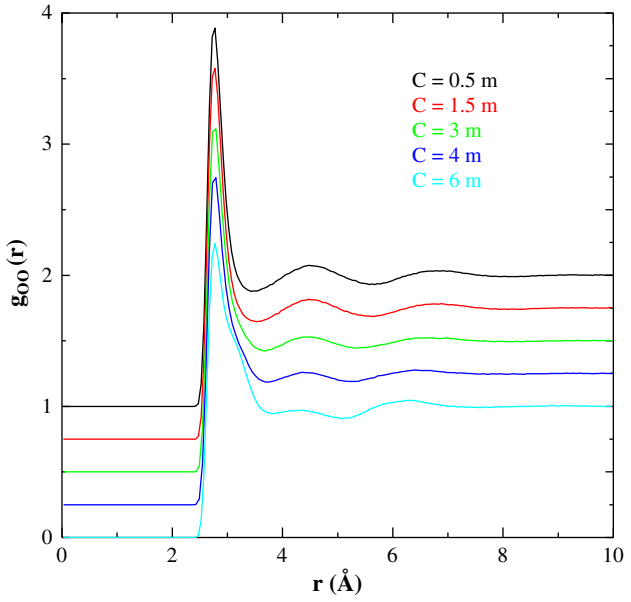


**Fig. 4.** The oxygen–oxygen pair correlation functions of aqueous LiCl solutions at different salt concentrations.

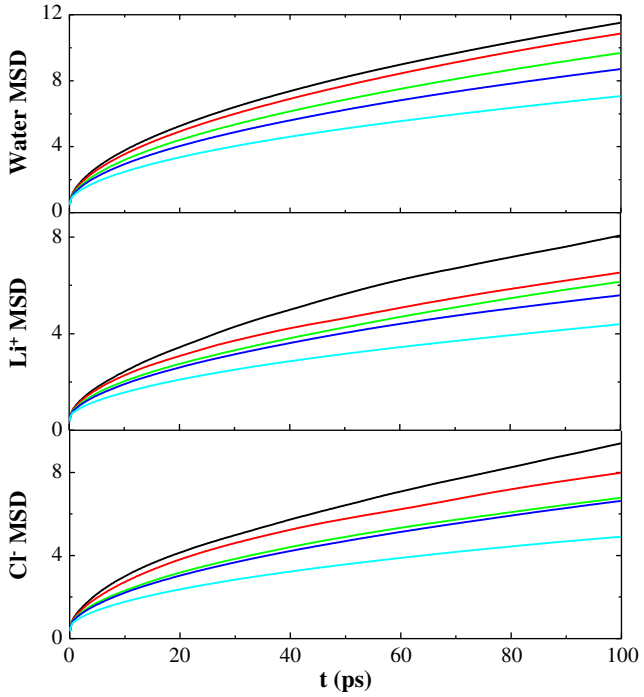


**Fig. 5.** Mean square displacement of the water, $Li^+$ and $Cl^-$ in aqueous LiCl solutions at 0.5, 1.5, 3, 4 and 6 m respectively from the top to the bottom.

In our previous study [21], related to aqueous NaCl solutions, we found that the self diffusion coefficients increase as the system size increases. Another aim of our investigations is then to study the trajectory length and the system-size effects on the dielectric constant. The effect of the trajectory length was investigated for the small system (256 particles/C = 3 m) and the average dielectric constant was calculated on every 1000-th configuration from 100 to 600 ps using the same time difference between consecutive configurations. As it can be seen from Fig. 8, there is no significant change of the dielectric constant calculated on every 1000 configurations from 100 to about 5000 ps. The same trend has been observed by Smith and Dang [32] in their study of pure fluid, using the same SPC/E potential. The convergence of the dielectric constant clearly appears from 6000 ps. In their study of aqueous lithium chloride solutions using SPC/E and SWM4-DP water models, Orolya and László [33] demonstrated that the trajectories shorter than about 5 ns are not applicable for providing a good estimate of the dielectric constant.

Otherwise, to study the system size effect, three different systems corresponding to C = 3 m and containing respectively 526, 1052 and 1536 particles were used. The calculated values of the dielectric constant derived from three systems are 50.674, 54.635 and 52.376 respectively at smallest to largest system. We can notice that the dielectric constant is a little sensitive to the system size since the difference between extrema is about 8%.

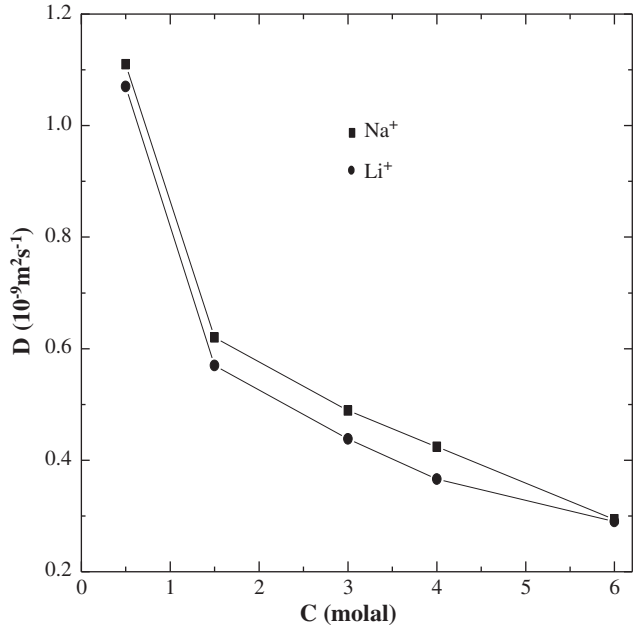


**Fig. 6.** Self diffusion coefficients of $Li^+$ and $Na^+$ respectively in LiCl and NaCl aqueous solutions at different salt concentrations.

**Table 3**
Self-diffusion coefficients of water molecules, $Li^+$ and $Cl^-$, calculated from the velocity autocorrelation functions and mean square displacements. The values of the reorientational correlation time of a unit vector $\vec{u}_\mu$ and the dielectric constant are also given.

| C/m | $D_W$ ($10^{-9}$ $m^2$ $s^{-1}$) | | $D_{Li+}$ ($10^{-9}$ $m^2$ $s^{-1}$) | | $D_{Cl-}$ ($10^{-9}$ $m^2$ $s^{-1}$) | | $\vec{u}_\mu$ direction | | $\varepsilon_S$ |
|---|---|---|---|---|---|---|---|---|---|
| | VACF | MSD | VACF | MSD | VACF | MSD | $\tau_\mu^1(ps)$ | $\tau_\mu^2(ps)$ | |
| C = 0.5 | 1.841 | 1.822 | 1.070 | 1.056 | 1.550 | 1.631 | 4.163 | 2.142 | 73.239 |
| C = 1.5 | 1.705 | 1.731 | 0.570 | 0.632 | 1.075 | 1.110 | 4.315 | 2.215 | 62.635 |
| C = 3 | 1.450 | 1.519 | 0.438 | 0.426 | 0.847 | 0.952 | 4.710 | 2.637 | 50.229 |
| C = 4 | 1.077 | 1.182 | 0.366 | 0.389 | 0.589 | 0.495 | 5.276 | 2.692 | 36.732 |
| C = 6 | 0.912 | 0.864 | 0.259 | 0.276 | 0.296 | 0.315 | 6.368 | 3.324 | 26.350 |

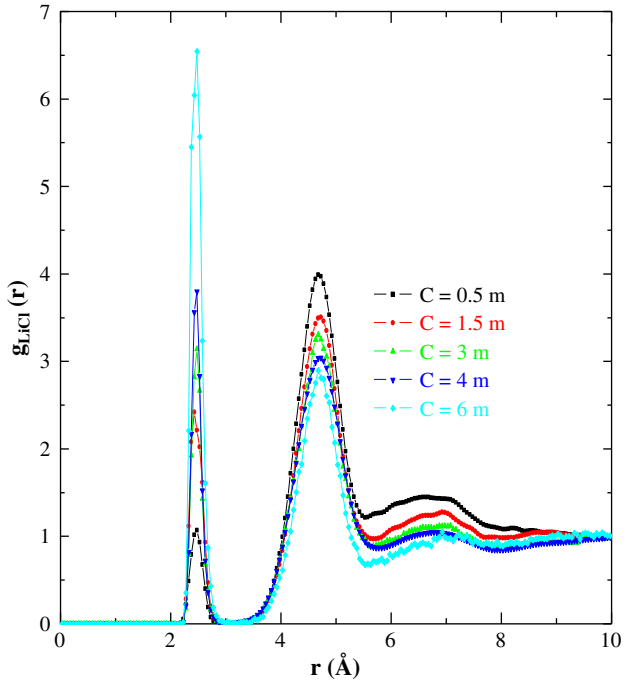


**Fig. 7.** The lithium–chlorine pair correlation functions of aqueous LiCl solutions at different salt concentrations.

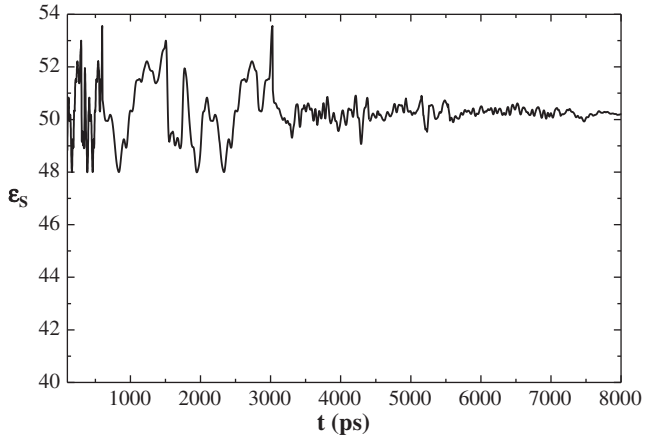


**Fig. 8.** The static dielectric constant for SPC/E water in LiCl aqueous solution at C = 3 m, as a function of simulation time.

## 4. Conclusion

In this study, we have presented structural and dynamical investigations of aqueous LiCl solutions at various salt concentrations ranging from 0.5 to 6 m. Computed structure factors of each system, using the SPC/E water model, largely agree with recently published x-ray ones. We have also found that the self diffusion coefficient decreases with increasing salt concentration. For higher salt concentration, the two diffusion coefficients for $Li^+$ and $Cl^-$ have been found quite close to each other, which can be explained by the formation of a cluster of these ions which tend to migrate together. Particularly the ratio of the first and the second reorientational correlation times differs from 3, which indicates the presence of angular jumps. As noted in Section 3, the calculated dielectric constant decreases with increasing salt concentration. This is possibly explained by the reduction of the reorientational correlation between water molecules in the vicinity of ions.

## References

[1] A.K. Soper, J. Phys. Condens. Matter 9 (1997) 2717.
[2] E. Guàrdia, D. Laria, J. Martí, J. Mol. Liq. 125 (2006) 107.
[3] I. Ohmine, H. Tanaka, Chem. Rev. 93 (1993) 2545.
[4] B. Bagchi, Chem. Rev. 105 (2005) 3197.
[5] S. Koneshan, J.C. Rasaiah, J. Chem. Phys. 113 (2000) 8125.
[6] D. Laage, J.T. Hynes, Science 311 (2006) 832.
[7] D. Laage, J.T. Hynes, Proc. Natl. Acad. Sci. 311 (2007) 11167.
[8] F. Canganella, A. Gambacorta, C. Kato, K. Horikoshi, Microbiol. Res. 154 (2000) 297.
[9] A. Shanableh, Water Res. 34 (2000) 945.
[10] N.J. Birch, Chem. Rev. 99 (1999) 2659.
[11] S. Bouazizi, S. Nasr, J. Mol. Struct. 837 (2007) 206.
[12] S. Bouazizi, S. Nasr, J. Mol. Struct. 875 (2008) 121.
[13] S. Bouazizi, S. Nasr, N. jaîdane, M.-C. Bellissent-Funel, J. Phys. Chem. B 110 (2006) 23515.
[14] H.J.C. Berendsen, J.R. Grigera, T.P. Straatsma, J. Phys. Chem. 91 (1987) 6269.
[15] S. Koneshan, J.C. Rasaiah, R.M. Lynden-Bell, S.H. Lee, J. Phys. Chem. B 102 (1998) 4193.
[16] S. Chowdhuri, A. Chandra, J. Chem. Phys. 118 (2003) 9719.
[17] J.P. Hansen, I.R. McDonald, Theory of Simple Liquids, Academic Press, London, 1976.
[18] S.W. de Leeuw, J.W. Perram, E.R. Smith, Proc. R. Soc. Lond. A 373 (1980) 27.
[19] H.J.C. Berendsen, J.P.M. Postma, W.F. Van Gunsteren, A. DiNola, J.R. Haak, J. Chem. Phys. 81 (1984) 3684.
[20] A.V. Egorov, A.V. Komolkin, V.I. Chizhik, P.V. Yushmanov, A.P. Lyubartsev, A. Laaksonen, J. Phys. Chem. B 107 (2003) 3234.
[21] S. Bouazizi, S. Nasr, J. Mol. Liq. 162 (2011) 78.
[22] S.H. Lee, J.C. Rasaiah, J. Phys. Chem. 100 (1996) 1420.
[23] S. Chowdhuri, A. Chandra, J. Chem. Phys. 115 (2001) 3732.
[24] I. Harsányi, Ph.A. Bopp, A. Vrhovšek, L. Pusztai, J. Mol. Liq. 158 (2011) 61.
[25] I. Harsányi, L. Temleitner, B. Beuneu, L. Pusztai, J. Mol. Liq. 165 (2012) 94.
[26] I. Harsányi, L. Pusztai, J. Chem. Phys. 137 (2012) 204503.
[27] J. Anderson, J. Ullo, S. Yip, Chem. Phys. Lett. 152 (1998) 447.
[28] P. Gallo, D. Corradini, M. Rovere, J. Mol. Liq. 189 (2014) 52.
[29] A. Glättli, X. Daura, W.F. van Gunsteren, J. Chem. Phys. 116 (2002) 9811.
[30] H. Behret, F. Schmithals, J. Barthel, Z. Phys. Chem. Neue Folge 96 (1975) 73.
[31] F. Franks (Ed.), Water — a Comprehensive Treatise, vols. 1, 3, Plenum, New York, 1973.
[32] D.E. Smith, L.X. Dang, J. Chem. Phys. 100 (1994) 3757.
[33] G. Orolya, P. László, Chem. Phys. Lett. 507 (2011) 80.